

A Search for the Standard Model Higgs Boson in the Process $ZH \rightarrow \ell^+\ell^- b\bar{b}$ Using 4.1 fb^{-1} of CDF II Data

The CDF Collaboration
<http://www-cdf.fnal.gov/>
 August 12, 2009

Abstract

We present a search for the standard model (SM) Higgs boson in the associated production process $p\bar{p} \rightarrow ZH \rightarrow \ell^+\ell^- b\bar{b}$ using 4.1 fb^{-1} of Tevatron data collected with the CDF II detector. We select events containing Z candidates reconstructed from e^+e^- or $\mu^+\mu^-$ pairs and containing at least two energetic jets. We form our final analysis sample by requiring events to contain at least one b -tagged jet. To enhance the discriminating power of the jet energies and associated quantities, we apply a neural network (NN) derived correction to the jets which depends on the missing transverse energy and its orientation with respect to the jets. We employ two dimensional NNs to simultaneously separate signal events from the dominant $Z + jets$ and $t\bar{t}$ backgrounds. These NNs use various kinematic distributions, matrix element probabilities and the output of a separate jet flavor separating NN as inputs. We find good agreement between the observed data and the predicted SM backgrounds and set 95% confidence level upper limits on the Higgs production cross section (σ_{ZH}) times the branching ratio for $H \rightarrow b\bar{b}$. For a Higgs boson mass of $115 \text{ GeV}/c^2$ we observe (expect) a 95% confidence level upper limit of 5.9 (6.8).

Preliminary Results

1 Introduction

The remaining unverified prediction of the standard model of particle physics (SM) is the existence of the Higgs boson, which is a by-product of spontaneous symmetry breaking under the Higgs mechanism [1]. The dominant SM Higgs process at the Tevatron is direct production through gluon-gluon fusion [2], with the Higgs subsequently decaying into a $b\bar{b}$ quark pair for $M_H \lesssim 135 \text{ GeV}/c^2$ or to a pair of oppositely charged W bosons for higher masses. Although the cross-sections for direct production are several times larger than Higgs production in association with a Z or W , the decay products of the Z/W (charged lepton(s)/ \cancel{E}_T) serve to distinguish Higgs events from multijet backgrounds. In this note we present the results of an updated search for the SM Higgs in the process $ZH \rightarrow \ell^+\ell^-b\bar{b}$. This analysis updates the previous search in 1 fb^{-1} [3] and expands upon the techniques developed for the (preliminary) searches preformed in 2.7 fb^{-1} [4, 5]. The following sections detail our event selection, data model, application of multivariate techniques, uncertainties and our results.

2 Event Selection

This search includes data recorded by the CDF II [6] Detector between February 2002 and February 2009 corresponding to an integrated luminosity of 4.1 fb^{-1} . We accept events selected by the inclusive CDF high P_T [7] lepton triggers which require one central ($|\eta| \leq 1.1$) muon candidate with $P_T \geq 18 \text{ GeV}/c$ or one central electron candidate with $E_T \geq 18 \text{ GeV}$. We also accept events from the CDF trackless trigger [8] which selects events containing two or more calorimeter deposits ($|\eta| \leq 3.6$) with $E_T \geq 18 \text{ GeV}$.

We select events containing two or more charged leptons of the same flavor (ee or $\mu\mu$) with the dilepton mass (M_{ll}) of the lead P_T pair falling in the mass window $76 \leq M_{ll} \leq 106 \text{ GeV}/c^2$. We impose an opposite charge requirement for all $\mu\mu$ and central-central (i.e. both electron candidates have $|\eta| \leq 1.1$) electron pairs. Events are further required to contain two or more jets (cone 0.4) with $E_T \geq 15 \text{ GeV}$ and $|\eta| \leq 2.0$. Jets meeting this requirement are referred to as “Tight Jets”. We further require that 1 or more of these jets have $E_T \geq 25 \text{ GeV}$.

Events meeting the above “*PreTag*” requirements satisfy the same kinematic selection as our final signal region and form a high statistics sample used to validate our analysis technique and data model. *PreTag* events are further divided into two categories (High $\frac{S}{B}$ and Low $\frac{S}{B}$) based upon the quality of the reconstructed Z candidate. In general, events containing a Z reconstructed from a $\mu\mu$ pair or a high quality central ($E_T \geq 18 \text{ GeV}$, Track $P_T \geq 9 \text{ GeV}/c$) electron and a lower quality ($E_T \geq 10 \text{ GeV}$) electron have low “*fake*” rates (discussed below) and enter the High $\frac{S}{B}$ category. An event passing only the trackless trigger or containing a Z candidate formed from the combination of a high quality central electron and a lower quality “*Crack – Track*” (track electron with $P_T \geq 20 \text{ GeV}/c$, with the track pointing to a non-instrumented region of the calorimeter) electron enter the Low $\frac{S}{B}$ category.

Our signal region sample is formed from *PreTag* events in which one or more of the jets are “*b*-tagged”. We use two different *b – tagging* algorithms to maximize signal acceptance :

- The secondary vertex (SecVtx) [9] tagging algorithm which tags *b* jets using displaced vertex information. We use both the ‘Tight’ and ‘Loose’ operating points.
- The jet probability (JP) [10] tagging algorithm which uses track impact parameters to compute the probability that a jet originated from the primary event vertex. We use the 5% operating point.

For each event in our *PreTag* sample, we first search for the presence of two or more tight SecVtx tagged jets. If two (or more) tight SecVtx tags are found, this event enters our double tag tight category (TT). If the event does not contain two tight SecVtx tagged jets, we search for one loose SecVtx tagged jet and a second jet with a jet probability value of ≤ 0.05 . Events meeting this requirement enter our loose + jet probability tag category (L+JP). If the event fails to enter the TT or L+JP categories, we then search for a single tight SecVtx tagged jet. Events that are not classified as TT or L+JP which contain a single tight SecVtx tagged jet enter our single tight tag category (T). We divide the final $Z + b$ -tagged jet sample into six sub-samples based on Z quality and the type of *b – tagging* algorithm(s) the jets satisfy. Our jet, *b – tag* requirements and signal region categories are summarized in Table 1.

Jet Selection for PreTag Region

2 or more Cone 0.4 jets with $E_T > 15$ GeV, $|\eta| < 2$
 1 of these jets with $E_T > 25$ GeV

| Signal Region | Z Quality | b-Tag Requirements |
|------------------|-----------|---|
| TT High | High S/B | 2 Tight SecVtx Tags |
| L+JP High | High S/B | 1 Loose SecVtx Tag & 1 JetProbability Tag |
| T High | High S/B | 1 Tight SecVtx Tags |
| | | |
| TT Low | Low S/B | 2 Tight SecVtx Tags |
| L+JP Low | Low S/B | 1 Loose SecVtx Tag & 1 JetProbability Tag |
| T Low | Low S/B | 1 Tight SecVtx Tags |

Table 1: Summary of jet selection and the final signal region categories.

3 Data Model

Background processes possessing a detector signature similar to the signal are mainly those which contain two leptons and two (or more) jets in the final state. The dominant background is $Z + jets$, with $Z +$ light flavor jets (u,d,s) forming the major background component before $b - tag$ requirements are imposed. $Z + jets$ events are modeled using an ALPGEN v2.10 prime MC [11] with PYTHIA [12] 6.325 for showering. Signal, diboson (ZZ, WZ, WW) and $t\bar{t}$ processes are modeled with PYTHIA 6.216 MC. The $t\bar{t}$ simulation assumes a top mass of $175 \text{ GeV}/c^2$.

The probability of a jet to 'fake' an electron is measured in independent jet triggered data samples (as a function of jet E_T) and applied to the jets in our selected events forming the "Fake" $Z \rightarrow ee$ contribution. The $Fake Z \rightarrow \mu\mu$ contribution is formed from events with like-sign muon pairs. The agreement between our model and observed

data is checked across a variety of kinematic distributions, some of which are shown in Figures 1 and 2. Table 2 lists the predicted number of events from major backgrounds and the number of observed events at PreTag.

After b -tag selection, the contribution from $Z +$ light flavor jets (Mistags) is modeled using re-weighted PreTag data events, with the weights reflecting the probability for a light flavor jet to be tagged as a b -jet. These probabilities are measured for each b -tag algorithm in independent jet triggered data samples.

| Source | PreTag High S/B | PreTag Low S/B |
|--|-----------------------|---------------------|
| tt | 53.01 ± 11.26 | 27.12 ± 5.76 |
| WW | 5.22 ± 0.71 | 4.3 ± 0.58 |
| WZ | 117.89 ± 15.95 | 27.04 ± 3.66 |
| ZZ | 118.14 ± 15.98 | 23.28 ± 3.15 |
| $Z \rightarrow \tau\tau$ | 2.98 ± 1.21 | 4.33 ± 1.76 |
| Z+jets (bb) | 370.93 ± 150.71 | 74.51 ± 30.28 |
| Z+jets (cc) | 682.59 ± 277.34 | 142.25 ± 57.79 |
| Z+jets (lf) | 9977.08 ± 1995.42 | 2206.9 ± 441.38 |
| fakes | 541.02 ± 270.51 | 504.44 ± 252.22 |
| ZH (120 GeV/c^2) | 4.25 ± 0.32 | 0.67 ± 0.05 |
| Total Background | 11868.9 ± 2038.4 | 3014.17 ± 512.6 |
| Data | 11806 | 3061 |

Table 2: Comparison of observed and predicted event totals for PreTag selection.

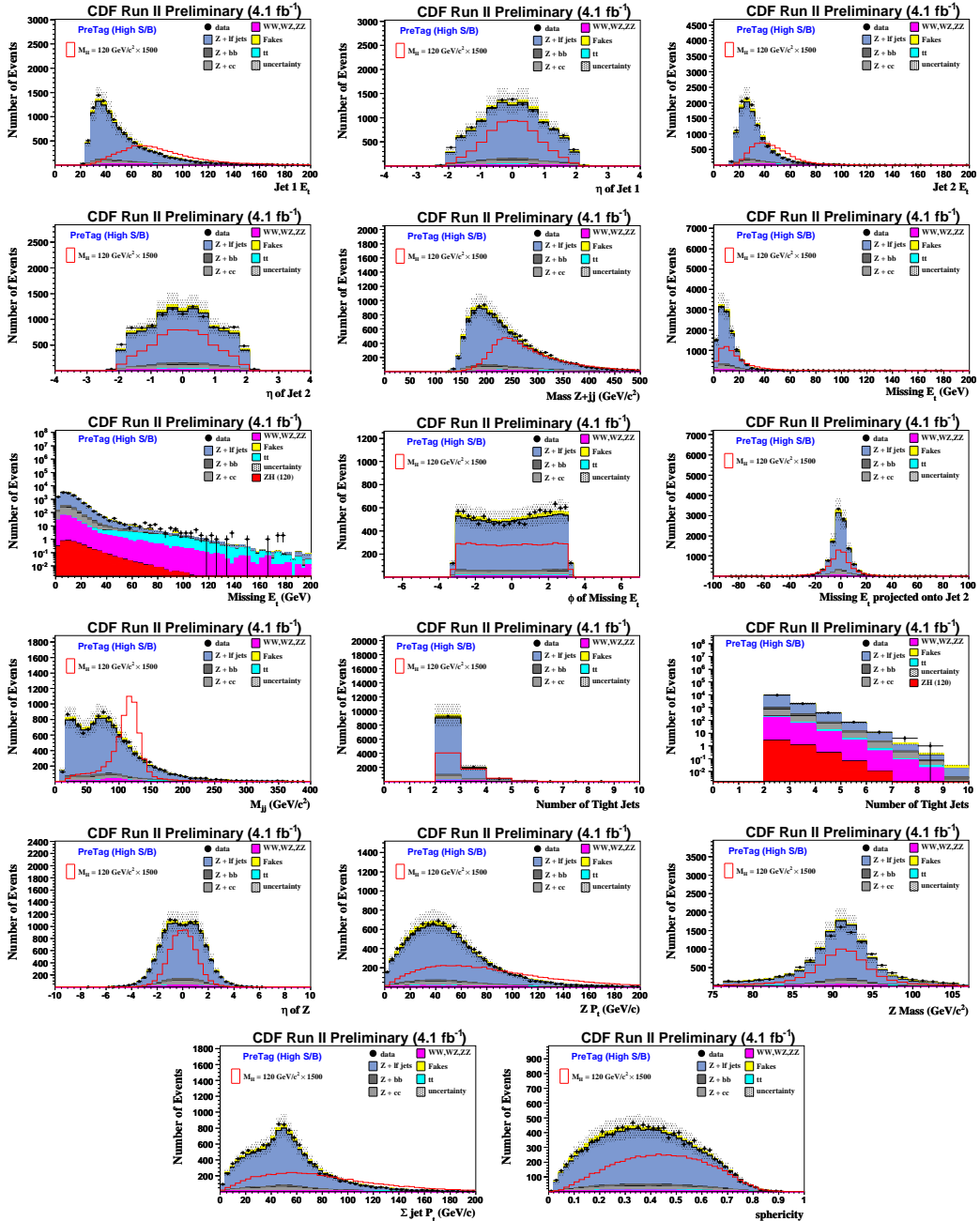


Figure 1: Selected distributions showing the agreement between our data and model for our PreTag High S/B selection.

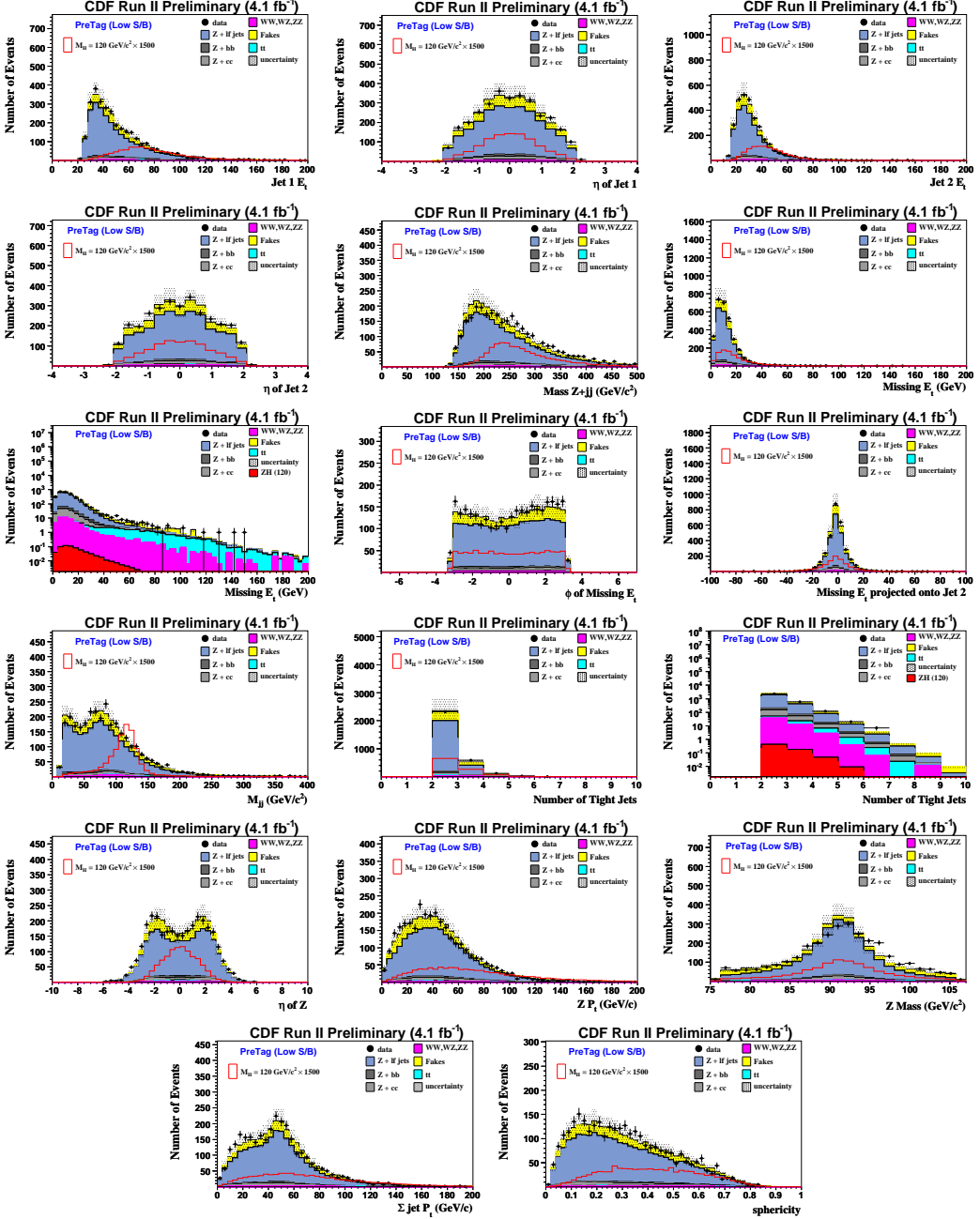


Figure 2: Selected distributions showing the agreement between our data and model for our PreTag Low S/B selection.

4 Multivariate Techniques

4.1 Jet Energy Corrections

The dijet mass (M_{jj}) is one of the most useful distributions for ZH vs. $Z + jets$ discrimination, with its separating power limited mainly by the jet energy resolution. In general, incorrect measurement of jet energies can result in over-estimation of the missing transverse energy (\cancel{E}_T). In order to improve the dijet mass resolution we correct the energies of the leading and second E_T jets by factors which depends on the direction and magnitude of the \cancel{E}_T , as well as its transverse projection onto the jets. The correction factors are the output values of an MLPfit [13] Neural Network derived function. All kinematic quantities (except for \cancel{E}_T) are computed using the NN corrected jet energies. The effect of these corrections on the dijet mass can be seen in Figure 3.

4.2 Flavor Separator NN

In previous iterations of this analysis the single tag categories have suffered from low S/B due to the presence of large ($\sim 40\%$) backgrounds from incorrectly tagged light flavor jet events. In order to increase the ability of our final analysis discriminants (2D-NN discussed below) to separate this “Mistag” background from signal, we include (as a potential) 2D-NN input, the output of the Karlsruhe Neural Network (KNN) $b - tagger$ [14]. The KNN is designed to separate b jets from c and light flavor jets.

4.3 Matrix Element Probabilities

In addition to kinematic distributions, we also consider matrix element probabilities (ME) as potential inputs to our final 2D-NNs. Matrix element discriminants were first employed in the search for $ZH \rightarrow \ell\ell b\bar{b}$ in [5] and are applied here with the same method of calculation. We compute matrix element probabilities for the processes $Z + jets$, $t\bar{t}$ and our signal.

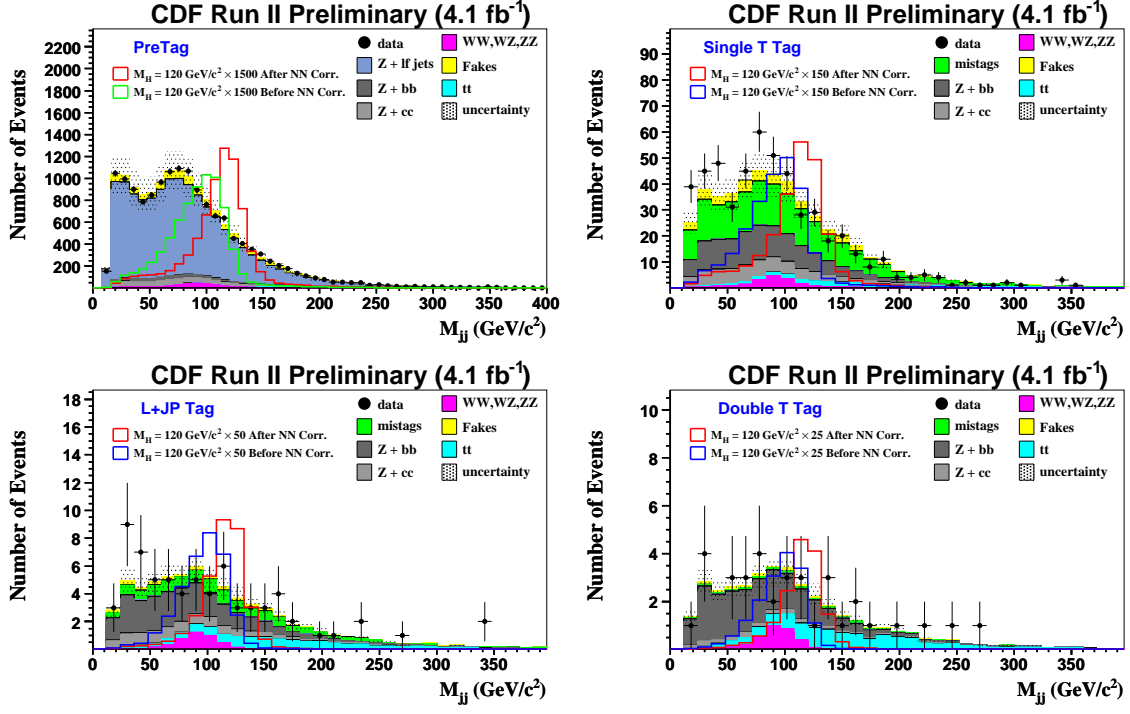


Figure 3: Effect of NN jet energy corrections on the dijet mass distributions.

4.4 Two Dimensional NNs for S/B Discrimination

The two largest background classes at tag level are $Z + jets$ like events (Zbb , fakes, Zcc , Mistags) and $t\bar{t}$. We train two dimensional JetNet [15] NNs to simultaneously separate signal events from $Z + jets$ and $t\bar{t}$. The NNs are designed to return two values (NNx, NNy) for a given sample. For signal the NN targets the values ($NNx = 1, NNy = 0$), for $Z + jets$ the NN targets ($NNx = 0, NNy = 0$) and for $t\bar{t}$, the target is ($NNx = 1, NNy = 1$). We optimize three NNs (one for each tag category) with each NN trained on the same sample of signal ($M_H = 120 \text{ GeV}/c^2$) and $t\bar{t}$ while the $Z + jets$ training samples are constructed to reflect the amount of light flavor, bb and cc events in each tag category.

We utilize a sequential input algorithm which automatically selects the most powerful discriminants as NN inputs. This algorithm begins by forming single input NNs

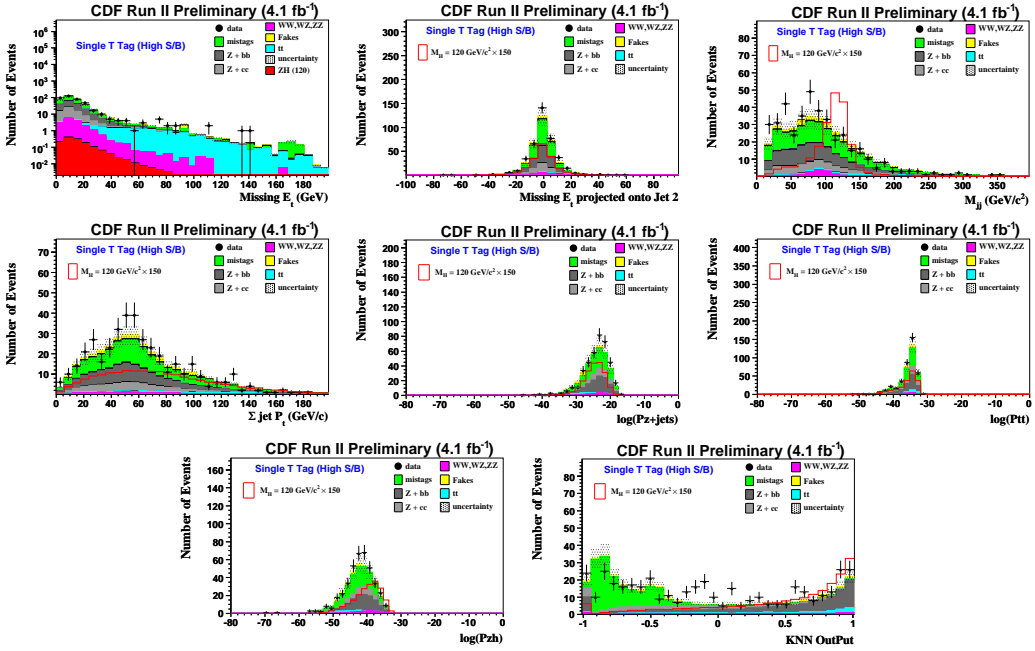


Figure 4: NN input distributions for the single tight tag category with high S/B selection.

(considering all ~ 40 available inputs) and finds the single input which produces the best performing (lowest testing error) NN. Once the best single input is found, the algorithm loops through the remaining pool of inputs to find the best two input NN. The algorithm continues in this way until the addition of inputs no longer improves the testing error. Once the algorithm has found the optimal inputs for each $b - tag$ category the final NNs are trained. The NN inputs can be seen in Figures 4 through 9.

5 Systematic Uncertainties

We assume a $\sim 5\%$ uncertainty on the integrated luminosity and we apply uncertainties of $4(T), 8(TT)$ and $11(L + JP)\%$ to our $b - tag$ MC samples to account for the systematic errors associated with the calculation of $b - tag$ efficiencies and scale factors. We apply 1% and 1.5% uncertainties on the trigger efficiency/lepton reconstruction and

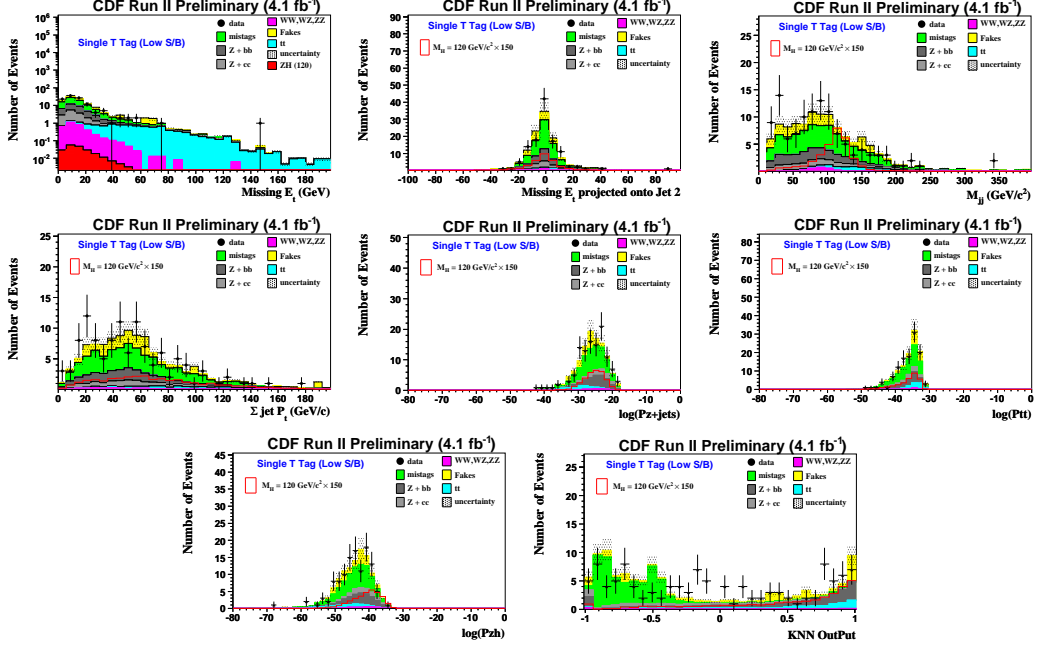


Figure 5: NN input distributions for the single tight tag category with low S/B selection.

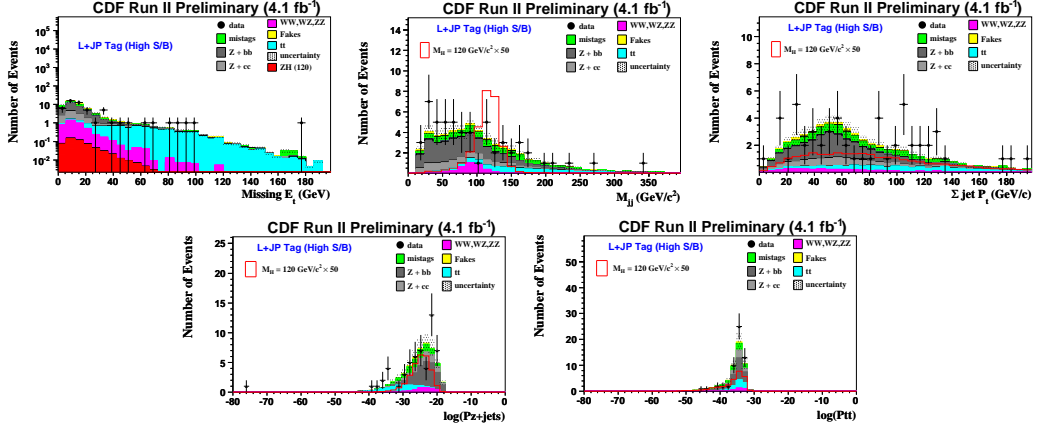


Figure 6: NN input distributions for the L+JP tag category with high S/B selection.

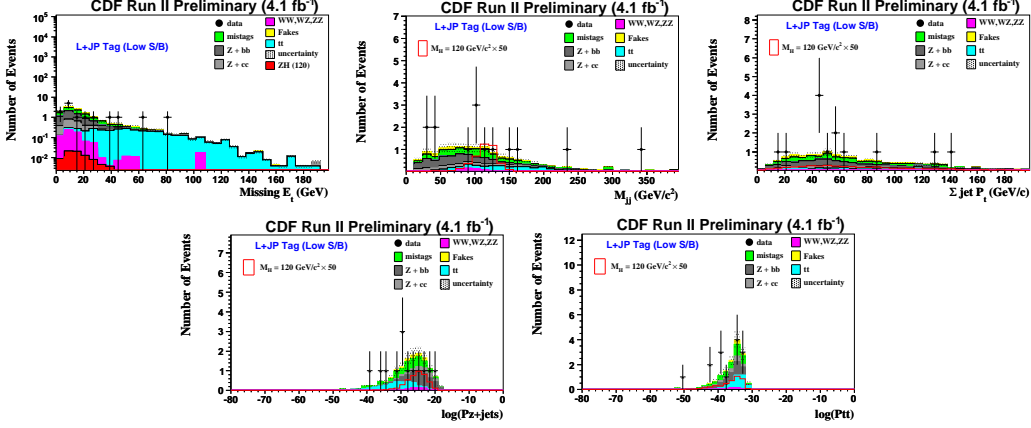


Figure 7: NN input distributions for the L+JP tag category with low S/B selection.

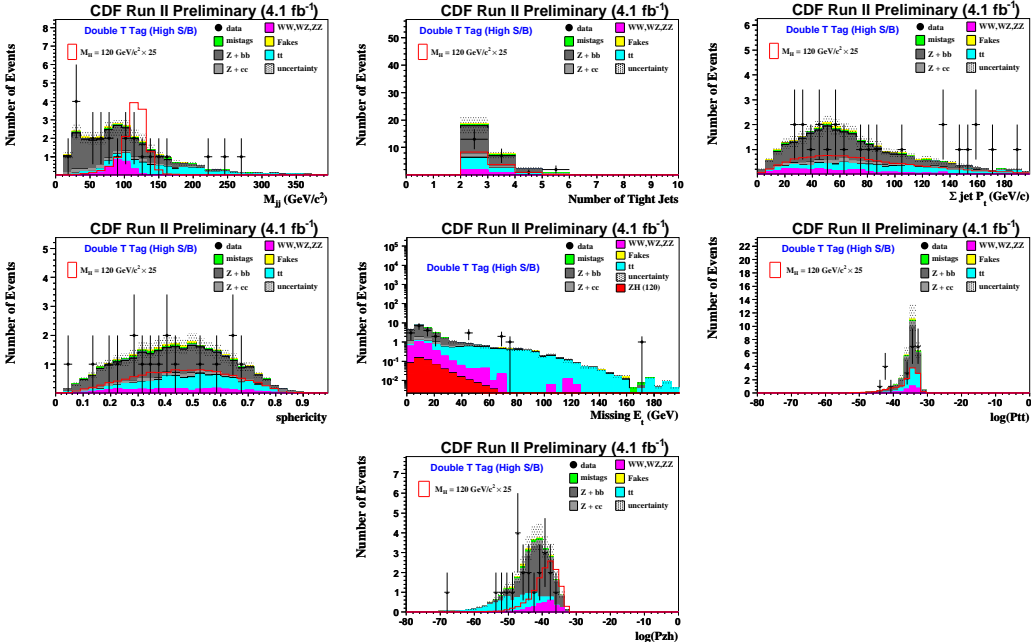


Figure 8: NN input distributions for the TT tag category with high S/B selection.

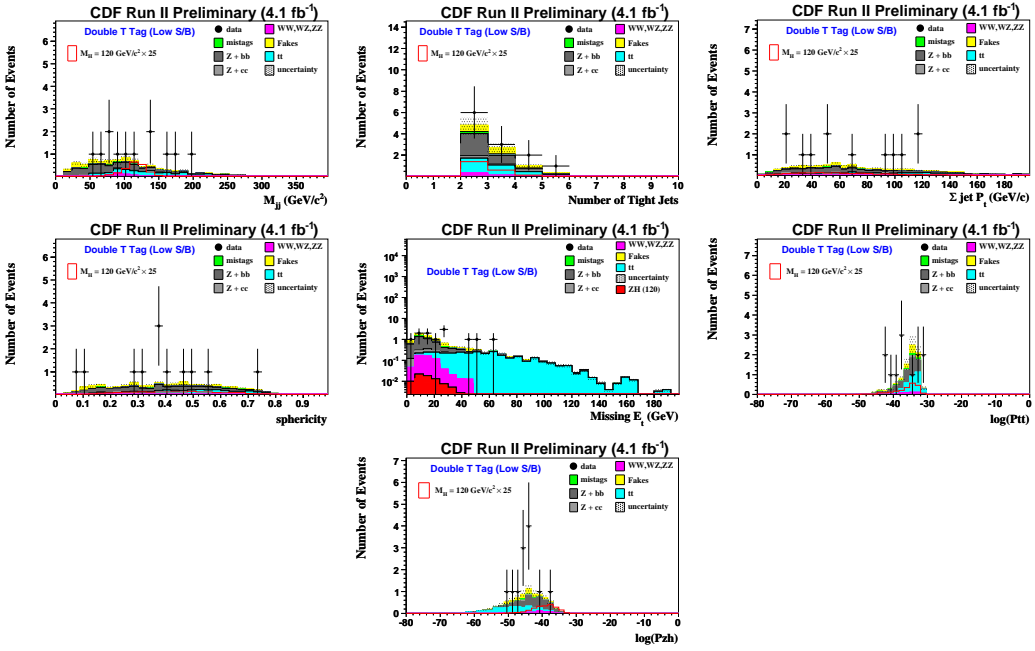


Figure 9: NN input distributions for the TT tag category with low S/B selection.

measured lepton energies. In order to cover the spread of fake rates measured from different jet triggered data samples we assign a 50% uncertainty on our total fake estimate. We apply a 40% uncertainty to $Z + bb$ and $Z + cc$ samples to cover the theoretical uncertainty on the $Z + \text{heavy flavor}$ jets cross-section. Similarly we apply an 11.5% cross-section uncertainty to all diboson samples, and 5% to signal. For $t\bar{t}$ we place a 20% uncertainty to account for both the theoretical uncertainty on the process cross-section and the difference between our simulated top mass ($175 \text{ GeV}/c^2$) and current experimental measurements. We also consider uncertainties which are expected to affect both sample normalizations and the shape of the NN output distributions, such as the jet energy scale (JES), the amount of initial/final state radiation (ISR/FSR) and the mistag event weights. Table 3 summarizes the systematic uncertainties applied in our limit calculations.

| systematic uncertainty | | Samples affected |
|--------------------------|------------------------------|--|
| Tevatron Luminosity | 0.05 | All MC |
| CDF Luminosity | 0.04 | All MC |
| $Z + h.f$ cross-section | 0.40 | $Z + bb, Z + cc$ |
| $t\bar{t}$ cross-section | 0.20 | $t\bar{t}$ |
| Diboson cross-sections | 0.115 | ZZ, ZW, WW |
| Mistag errors | NN Output Shape & Acceptance | Mistags |
| Lepton ID | 0.01 | All MC |
| B-tag scale factor | 0.04 0.08 0.11 | All single tag MC All double SecVtx tag MC All Loose + JP tag MC |
| Fakes | 0.50 | Fake $ee, \mu\mu$ |
| JES | NN Output Shape & Acceptance | All MC |
| ISR & FSR | NN Output Shape & Acceptance | Signal MC |
| ZH cross-section | 0.05 | ZH MC |
| EM energy scale | 0.015 | All MC |

Table 3: Summary of systematic uncertainties in terms of fractional acceptance change on samples.

6 Results

After applying b -tag selection, our final event totals are shown in tables 4 and 5. The projected NN output distributions for the signal regions are shown in Figure 6. We do not observe a significant excess over the number of events predicted by our background model and proceed to set limits on the maximum allowed ZH contribution to the data. We use the MCLIMIT [16] machinery to set 95% confidence level upper limits on $\sigma_{ZH} \times BR(H \rightarrow b\bar{b})$ and compute observed limits for Higgs masses between 100 and 150 GeV/ c^2 in 5 GeV intervals. Tables 6 and 7 and Figure 6 show our expected and observed limits for ZH production.

| Source | (High S/B Categories) | | |
|--------------------------------------|-------------------------|-----------------|------------------|
| | Double T Tag | L+JP Tag | Single T Tag |
| tt | 7.0 ± 1.5 | 8.1 ± 1.9 | 17.3 ± 3.6 |
| WW | 0.02 ± 0.003 | 0.1 ± 0.01 | 0.2 ± 0.03 |
| WZ | 0.1 ± 0.01 | 0.5 ± 0.1 | 4.8 ± 0.7 |
| ZZ | 2.7 ± 0.4 | 3.4 ± 0.6 | 11.1 ± 1.5 |
| Z+jets (bb) | 16.1 ± 6.8 | 21.5 ± 9.2 | 105.4 ± 44.3 |
| Z+jets (cc) | 1.8 ± 0.7 | 8.0 ± 3.3 | 53.7 ± 22.6 |
| Z+Mistags | 0.9 ± 0.3 | 9.4 ± 3.2 | 151.6 ± 22.7 |
| fakes | 0.7 ± 0.3 | 1.8 ± 0.9 | 22.0 ± 11.0 |
| ZH (120 GeV/c^2) | 0.5 ± 0.1 | 0.6 ± 0.1 | 1.4 ± 0.1 |
| Total Background | 29.3 ± 7.0 | 52.8 ± 10.5 | 366.1 ± 55.9 |
| Data | 23 | 56 | 406 |

Table 4: Comparison of observed and predicted event totals for tag level high S/B selection.

7 Conclusions

We have evaluated new limits with an updated dataset, ~ 4 times larger than in the previous (1 fb^{-1} published) analysis. We have incorporated the expanded selection implemented in the 2.4 and 2.7 fb^{-1} NN searches, and from the matrix element searches performed in 2.0 and 2.7 fb^{-1} we have added the matrix element discriminants. In addition to combining previous improvements, we have added new techniques including the use of the Karlsruhe flavor separator and the optimization of separate NNs for each tag category. We calculate 95% confidence level upper limits from 6.34 to 73.72 times the Standard Model prediction for Higgs Boson masses between $100\text{ GeV}/c^2$ and $150\text{ GeV}/c^2$. For $m_H = 115\text{ GeV}/c^2$ the expected 95% confidence level upper limit is 6.8 times the Standard Model prediction with an observed limit of 5.91 .

| Source | (Low S/B Categories) | | |
|-----------------------------------|------------------------|------------------|------------------|
| | Double T Tag | L+JP Tag | Single T Tag |
| tt | 2.9 ± 0.6 | 3.2 ± 0.8 | 8.9 ± 1.9 |
| WW | | 0.02 ± 0.003 | 0.1 ± 0.02 |
| WZ | | 0.1 ± 0.02 | 1.2 ± 0.2 |
| ZZ | 0.5 ± 0.1 | 0.5 ± 0.1 | 2.0 ± 0.3 |
| Z+jets (bb) | 3.2 ± 1.4 | 4.0 ± 1.7 | 21.1 ± 8.9 |
| Z+jets (cc) | 0.3 ± 0.1 | 1.6 ± 0.7 | 11.0 ± 4.6 |
| Z+Mistags | 0.4 ± 0.1 | 3.8 ± 1.3 | 50.0 ± 7.5 |
| fakes | 1.4 ± 0.7 | 1.1 ± 0.5 | 22.5 ± 11.3 |
| ZH (120 GeV/c²) | 0.1 ± 0.01 | 0.1 ± 0.02 | 0.2 ± 0.03 |
| Total Background | 8.7 ± 1.7 | 14.3 ± 2.4 | 116.8 ± 17.0 |
| Data | 12 | 14 | 116 |

Table 5: Comparison of observed and predicted event totals for tag level low S/B selection. Blank entries denote negligible contributions.

References

- [1] Peter W. Higgs. Broken symmetries and the masses of gauge bosons. *Phys. Rev. Lett.*, 13:508–509, 1964.
- [2] A. Stange, William J. Marciano, and S. Willenbrock. Higgs bosons at the Fermilab Tevatron. *Phys. Rev.*, D49:1354–1362, 1994.
- [3] T. Aaltonen et al. Search for the Higgs boson produced with $Z \rightarrow \ell^+\ell^-$ in $p\bar{p}$ collisions at $\sqrt{s} = 1.96$ TeV. *Phys. Rev. Lett.*, 101:251803, 2008.
- [4] Richard Hughes, Ben Kilminster, Brandon Parks, Brian Winer, Rob Harr, Shalhout Shalhout, Bo Jayatilaka, Ashutosh Kotwal, Ravi Shekhar, and Daniel White-

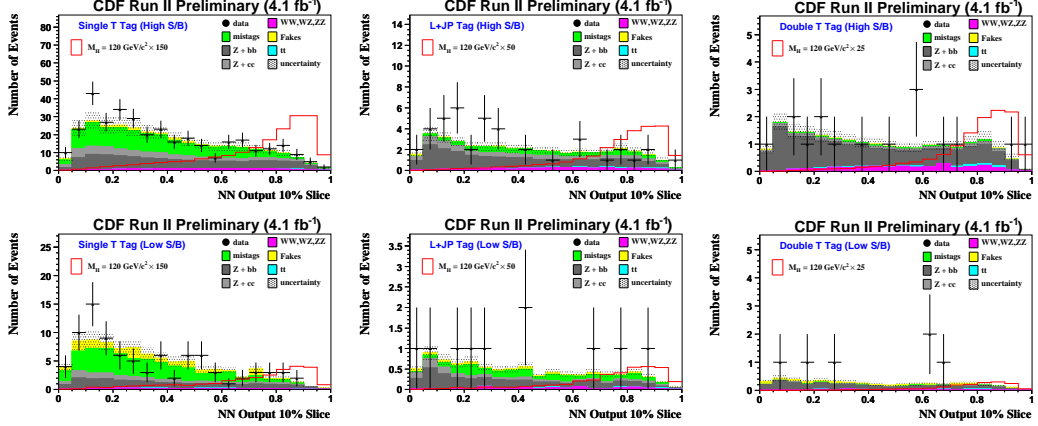


Figure 10: NN output distributions for b -tagged events. These are projections of two dimensional NN outputs, with a cut made ($NN_y < 0.1$) to highlight the most signal like region.

son. A Search for $ZH \rightarrow llbb$ in 2.7 fb^{-1} using a Neural Network Discriminant. *CDF Public Note 9665*.

- [5] Richard Hughes, Ben Kilminster, Brandon Parks, Brian Winer, Rob Harr, Shalhout Shalhout, Bo Jayatilaka, Ashutosh Kotwal, Ravi Shekhar, and Daniel Whiteson. A Search for $ZH \rightarrow llbb$ in 2.7 fb^{-1} using the Matrix-Element Method. *CDF Public Note 9718*.
- [6] D. Acosta et al. Measurement of the $t\bar{t}$ production cross section in $p\bar{p}$ collisions at $\sqrt{s} = 1.96 \text{ TeV}$ using lepton + jets events with secondary vertex b -tagging. *Phys. Rev. D*, 71(5):052003, Mar 2005.
- [7] We use a cylindrical coordinate system with z along the proton beam direction, r the perpendicular radius from the central axis of the detector, and ϕ the azimuthal angle. For θ the polar angle from the proton beam, we define $\eta = -\ln \tan(\theta/2)$. P_T refers to transverse momentum, while E_T denotes transverse energy.

| Expected and Observed Limits | | |
|------------------------------|-----------------------------------|----------|
| M_H | Expected $^{+1\sigma}_{-1\sigma}$ | Observed |
| 100 | 6.7 \pm 2.91 2.18 | 4.53 |
| 105 | 6.38 \pm 2.67 1.94 | 4.6 |
| 110 | 6.34 \pm 3.17 1.9 | 5.25 |
| 115 | 6.8 \pm 3.22 2.04 | 5.91 |
| 120 | 8.49 \pm 3.58 2.57 | 7.89 |
| 125 | 10.21 \pm 3.99 3.18 | 8.14 |
| 130 | 12.79 \pm 6.27 3.9 | 10.3 |
| 135 | 18.74 \pm 8.34 5.79 | 14.41 |
| 140 | 28.49 \pm 12.22 8.67 | 19.27 |
| 145 | 45.34 \pm 18.76 13.31 | 24.22 |
| 150 | 73.72 \pm 37.3 23.07 | 42.93 |

Table 6: Expected and observed limits.

- [8] This trigger fires on events with two or more calorimeter deposits of $E_T \geq$ GeV and $|\eta| \leq 3.6$. Unlike the CDF high P_T lepton triggers, this trigger does not require the calorimeter deposits to be matched to a track.
- [9] Robert Duane Harrington. Measurement of the top quark mass in lepton+jets events with secondary vertex tagging. FERMILAB-THESIS-2007-25.
- [10] A. Abulencia et al. Measurement of the $t\bar{t}$ Production Cross Section in $p\bar{p}$ collisions at $\sqrt{s} = 1.96$ -TeV using Lepton + Jets Events with Jet Probability b^- tagging. *Phys. Rev.*, D74:072006, 2006.

CDF Run II Preliminary (4.1 fb⁻¹)

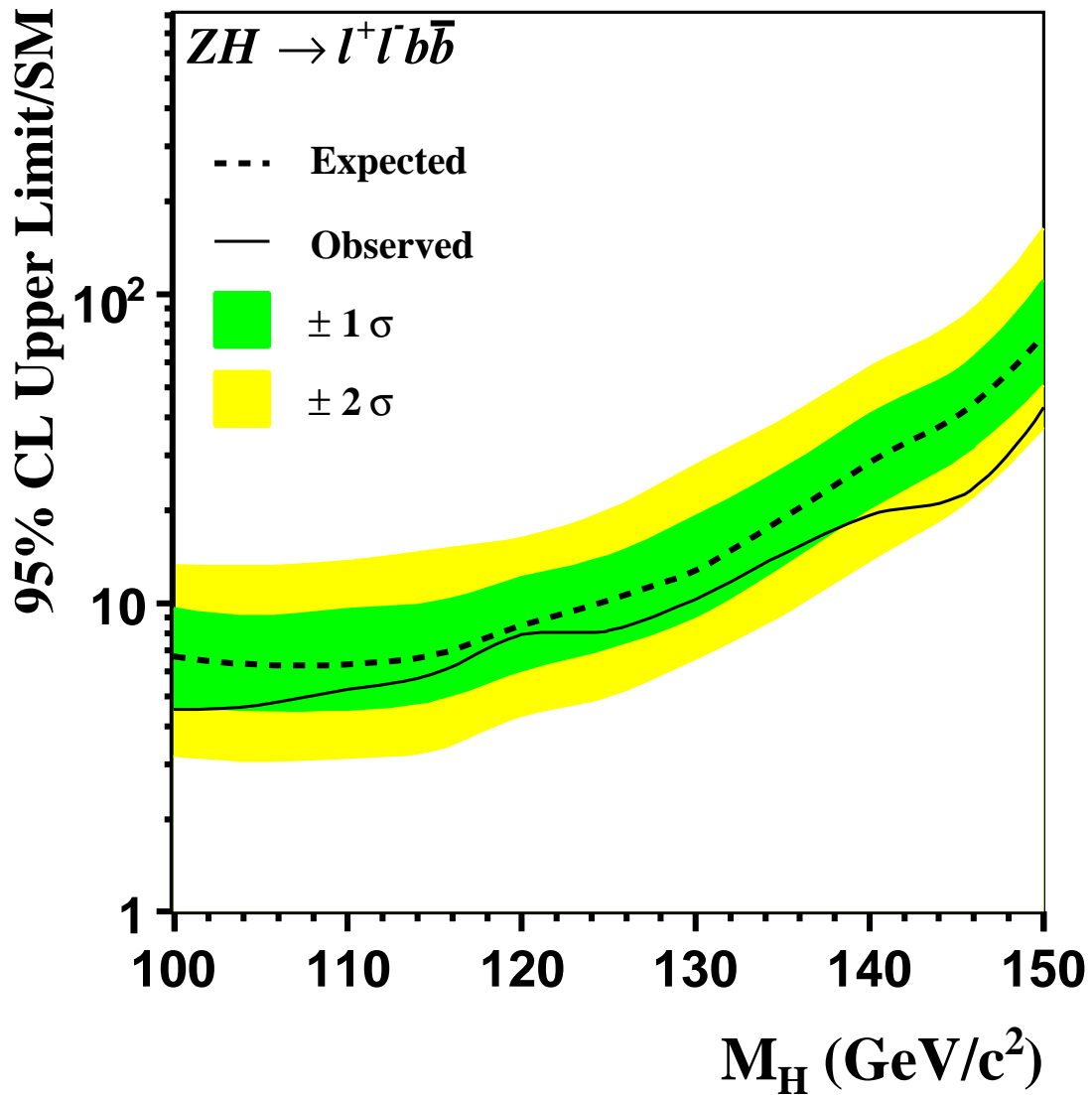


Figure 11: Expected and observed 95% CL upper limits on $\sigma_{ZH} \times BR(H \rightarrow b\bar{b})$.

**Expected and Observed 95% CL Upper Limits for
Individual Channels @ $M_H = 115 \text{ GeV}/c^2$**

| Channel | Data | Background | S/\sqrt{B} | Expected $^{+1\sigma}_{-1\sigma}$ | Observed |
|----------------------------|------|------------------|--------------|-----------------------------------|----------|
| Double Tag High S/B | 23 | 29.3 ± 7.0 | 0.13 | 12.1 ± 5.5 | 11.3 |
| L+JP Tag High S/B | 56 | 52.8 ± 10.5 | 0.09 | 15.98 ± 6.95 | 10.6 |
| Single Tag High S/B | 406 | 366.1 ± 55.9 | 0.09 | 15.5 ± 7.98 | 16.9 |
| Double Tag Low S/B | 12 | 8.7 ± 1.7 | 0.04 | 49.2 ± 19.9 | 58.2 |
| L+JP Tag Low S/B | 14 | 14.3 ± 2.4 | 0.03 | 50.6 ± 21.6 | 71.1 |
| Single Tag Low S/B | 116 | 116.8 ± 17.0 | 0.02 | 41.6 ± 20.04 | 38.5 |
| Combined | | | | 6.8 ± 3.22 | 5.91 |

Table 7: Expected and observed limits for individual channels.

- [11] Michelangelo L. Mangano, Fulvio Piccinini, Antonio D. Polosa, Mauro Moretti, and Roberto Pittau. ALPGEN, a generator for hard multiparton processes in hadronic collisions. *Journal of High Energy Physics*, Issue 07, pp. 001, 2003.
- [12] T. Sjöstrand, P. Edén, C. Friberg, L. Lönnblad, G. Miu, S. Mrenna, and E. Norrbinand. High-Energy-Physics Event Generation with PYTHIA 6.1. *Computer Phys. Commun.*, 135, 2001.
- [13] <http://schwind.home.cern.ch/schwind/MLPfit.html>.
- [14] Michael Feindt, Thomas Muller, Svenja Richter, and Wolfgang Wagner. A Neural Network b Tagger for Single-Top Analyses. *CDF Internal Note 7816*.

- [15] Carsten Peterson, Thorsteinn Rognvaldsson, and Leif Lonnblad. JETNET 3.0: A Versatile artificial neural network package. *Comput. Phys. Commun.*, 81:185–220, 1994.
- [16] Thomas Junk. Confidence Level Computation for Combining Searches with Small Statistics. *Nucl. Instrum. Meth.*, A434:435–443, 1999.